

The galaxy counterpart and environment of the dusty damped Lyman- α absorber at $z = 2.226$ towards Q 1218+0832

J. P. U. Fynbo^{1,2}, L. Christensen^{1,2}, S. J. Geier^{3,4}, K. E. Heintz^{1,2}, J.-K. Krogager⁵, C. Ledoux⁶, B. Milvang-Jensen^{1,2}, P. Møller⁷, S. Vejlggaard^{1,2}, J. Viuhon^{1,2}, G. Östlin⁸

¹ Cosmic DAWN Center, e-mail: jfynbo@nbi.ku.dk

² Niels Bohr Institute, University of Copenhagen, Jagtvej 155, 2200 Copenhagen N, Denmark

³ Instituto de Astrofísica de Canarias, Vía Láctea, s/n, 38205, La Laguna, Tenerife, Spain

⁴ Gran Telescopio Canarias (GRANTECAN), 38205 San Cristóbal de La Laguna, Tenerife, Spain

⁵ Université Lyon1, ENS de Lyon, CNRS, Centre de Recherche Astrophysique de Lyon UMR5574, F-69230 Saint-Genis-Laval, France

⁶ European Southern Observatory, Alonso de Córdova 3107, Vitacura, Casilla 19001, Santiago, Chile

⁷ European Southern Observatory, Karl-Schwarzschildstrasse 2, D-85748 Garching, Germany

⁸ Department of Astronomy, Oscar Klein Centre, Stockholm University, AlbaNova universitetscentrum, SE-106 91 Stockholm, Sweden

Received 2023; accepted, 2023

ABSTRACT

We report on further observations of the field of the quasar Q 1218+0832. Geier et al. 2019 presented the discovery of the quasar resulting from a search for quasars reddened and dimmed by dust in foreground damped Lyman- α absorbers (DLAs). The DLA is remarkable by having a very large H I column density close to 10^{22} cm⁻². Its dust extinction curve shows the 2175Å bump known from the Local Group. It also shows absorption from cold gas exemplified by C I and CO molecules. For this paper, we present narrow-band observations of the field of Q 1218+0832 and also use an archival Hubble Space Telescope (HST) image to search for the galaxy counterpart of the DLA. No emission from the DLA galaxy is found in either the narrow-band imaging or in the HST image. In the HST image, we could probe down to an impact parameter of 0.3 arcsec and a 3- σ detection limit of 26.8 mag per arcsec². In the narrow-band image, we probed down to a 0 arcsec impact parameter and detected nothing down to a 3- σ detection limit of about 3×10^{-17} erg s⁻¹ cm⁻². We did detect a bright Lyman- α emitter 59 arcsec south of Q 1218+0832 with a flux of 3×10^{-16} erg s⁻¹ cm⁻². We conclude that the DLA galaxy must be located at a very small impact parameter (<0.3 arcsec, 2.5 kpc) or it is optically dark. Also, the DLA galaxy most likely is part of a galaxy group.

Key words. quasars: general – quasars: absorption lines – quasars: individual: Q 1218+0832

1. Introduction

Considerations about the nature of the first galaxies go back at least to the 1960s. Partridge & Peebles (1967) argued that the first galaxies ought to be very bright in redshifted Lyman- α emission. Some searches were conducted, but except for the quasars discovered in 1963 (Schmidt 1963) and other active galactic nuclei, no 'normal' galaxies were discovered at redshifts $z > 2$ (e.g. Koo 1986). In 1986, a breakthrough resulted from the realisation that normal galaxies could be identified as damped Lyman- α absorbers (DLAs) and studied in absorption against the light of background quasars (Wolfe et al. 1986). DLAs were detected as broad absorption lines in the Lyman- α forest with neutral hydrogen column densities in excess of 2×10^{20} cm⁻² similar to what is measured in the gaseous disks of local spiral galaxies. The first such object was discovered in a quasar spectrum already in 1972 (Beaver et al. 1972), but at that time their nature as intervening galaxies was not fully realised. Even today, DLAs remain the most important class of objects for tracing cosmic chemical evolution in detail for a large range of chemical elements (e.g. Lu et al. 1996; Wolfe et al. 2005; Péroux & Howk 2020).

The study of $z > 2$ galaxies in emission progressed slower than the absorption studies. Only very few of the galaxies caus-

ing DLAs could be detected by their own light (e.g. Møller & Warren 1993, and references therein). In 1996 the observational study of the first galaxies was revolutionised by the discovery, largely driven by the advent of 8-10 m class telescopes, of the so-called Lyman break or drop-out galaxies (Steidel et al. 1996) and in a sense the current plethora of discoveries of galaxies at $z > 6$ is a consequence and unfolding of this 1996 breakthrough.

Now with 50 years having passed since their discovery, there has been great progress in understanding the nature of DLAs and their relation to galaxies detected in emission. Around the turn of the millennium, it was realised that the difficulty in detecting DLA galaxies in emission most likely had to do with the steepness of the galaxy distribution function. Most of the DLAs must be caused by dwarf galaxies below the detection limit of galaxy surveys (Fynbo et al. 1999; Haehnelt et al. 2000; Schaye 2001). This was somewhat disconcerting as this meant that galaxies studied in absorption and in emission would remain almost disjoint samples. Avenues for progress returned when it was realised that metallicity-luminosity and metallicity-mass correlations most likely were already established at $z > 2$ and were valid for absorption-selected galaxies too (Møller et al. 2004; Ledoux et al. 2006; Christensen et al. 2014). Based on the simple model in Fynbo et al. (2008), an observing strategy for detecting DLA

galaxies in emission was designed and that led to a substantial increase in the number of detections (Fynbo et al. 2010, 2013; Noterdaeme et al. 2012; Krogager et al. 2017). Subsequently, galaxy counterparts of metal-rich DLAs have also been detected in emission at sub-millimetre wavelengths (e.g. Neeleman et al. 2017; Møller et al. 2018; Kanekar et al. 2020; Kaur et al. 2022). The use of Integral Field Units has also resulted in more detections in H- α and Lyman- α emission (P  roux et al. 2011; Jorgenson & Wolfe 2014; Mackenzie et al. 2019; Lofthouse et al. 2023).

The focus on metal-rich DLAs rejuvenated the discussion of dust bias in connection with DLAs. Since most quasars have been selected based on their optical colours, it is unavoidable for the most dusty and metal-rich DLAs, due to dimming and reddening of the background quasars, to be under-represented (Ostriker & Heisler 1984; Pei et al. 1999; Wild & Hewett 2005). Krogager et al. (2019) show, through detailed simulations of quasar selection and the effect of dust in DLAs, that the cosmic density of metals may well be underestimated by as much as a factor of 5 at redshifts around 2.5 due to dust bias. Such a large uncertainty poses a serious problem when it comes to mapping cosmic chemical evolution and establishing the connection between DLAs and galaxies observed in emission. We have therefore worked on various ways to search for these missing quasars that otherwise have evaded normal quasar selection techniques due to reddening caused by dust in foreground DLAs (e.g. Fynbo et al. 2013; Krogager et al. 2016a). Other teams used radio selection to try to circumvent the dust bias of optically selected quasar surveys (e.g. Ellison et al. 2001; Jorgenson et al. 2006; Sadler et al. 2020; Gupta et al. 2021).

In this paper, we present new data for one such system, namely the striking example of the $z = 2.226$ DLA towards the $z = 2.60$ Q 1218+0832 (for other examples see Krogager et al. 2016b; Fynbo et al. 2017; Heintz et al. 2018). In Geier et al. (2019) (paper I hereafter), the discovery of the quasar and the characterisation of the DLA in terms of H I column density and other absorption lines based on low-resolution ($\lambda/\Delta\lambda = 500 - 1680$) spectroscopy is described. The DLA has a very large column density close to $10^{21.95\pm 0.15} \text{ cm}^{-2}$ and has absorption from both neutral carbon and CO molecules (due to the low resolution, column densities for these lines could not be determined). From the low-resolution spectrum, a lower limit of 10% solar was placed on the metallicity (based on Zn II lines). The dust extinction curve shows the presence of the 2175-   bump known from the Milky Way extinction curve (Stecher 1965). The reddening was determined to be $A_V = 0.82 \pm 0.02$ mag assuming $z = 2.2261$ for the location of the dust. We have not yet managed to secure a high-resolution spectrum of Q 1218+0832, which would allow precise measurement of the metallicity and the column densities of molecules. Instead of pursuing this approach, our paper focusses on describing new observations of the field using narrow-band imaging. The primary objective of these observations was to search for the galaxy counterpart of the DLA and other Lyman- α emitting galaxies in its environment. Furthermore, we analysed public imaging data obtained with the Hubble Space Telescope (HST) that happen to cover the position of Q 1218+0832. These observations allowed us to search for broad-band emission from a galaxy counterpart down to small impact parameters (a few kiloparsecs).

The paper is organised in the following way. In Sect. 2, we present our observations and briefly describe the data reduction. In Sect. 3, we present our results, which we discuss in the context of the related results from other teams in Sect. 4. In Sect. 5, we present our conclusions. In the paper we assume a flat Λ CDM

cosmology with $H_0 = 70 \text{ km s}^{-1} \text{ Mpc}^{-1}$, $\Omega_\Lambda = 0.7$, and $\Omega_m = 0.3$.

2. Observations and data reduction

We have previously used the Nordic Optical Telescope (NOT) for narrow-band-based searches for galaxies at redshift $z \approx 2$ (e.g. Fynbo et al. 1999, 2002). Such studies take a long time to prepare as special filters have to be designed and procured for each target. However, we realised that a 63  -wide filter (named NB391_7) made for other purposes (Sandberg et al. 2015) already exists in the NOT filter set, which by chance is perfectly suited for a study of the $z = 2.226$ DLA towards Q 1218+0832 (see Fig. 1). In March 2023 we carried out a pilot study (in the sense that we have not reached the detection limit we ultimately would like to reach) of the field using the SDSS g and r filters (g and r hereafter) and the NB391_7 filter in a 3-night observing with the NOT equipped with the Alhambra Faint Object Spectrograph and Camera (ALFOSC). One night was lost to bad weather, but we managed to get data on two other nights with clear sky conditions and seeing between 1 and 1.5 arcsec.

We also secured spectroscopic observations of an emission line source discovered in the ALFOSC imaging as described in Sect. 3. Those observations were obtained with the Optical System for Imaging and low-Intermediate-Resolution Integrated Spectroscopy (OSIRIS) at the Gran Telescopio Canarias (GTC). We used the R1000B grism and a 1.23 arcsec-wide slit providing a resolution of $\lambda/\Delta\lambda = 500$ and a wavelength coverage of 3600–7770   . The spectrum was taken at a high airmass of 2.0, as the object was only observable briefly at the beginning of the night, but otherwise under excellent observing conditions.

The log of observations can be seen in Table 1.

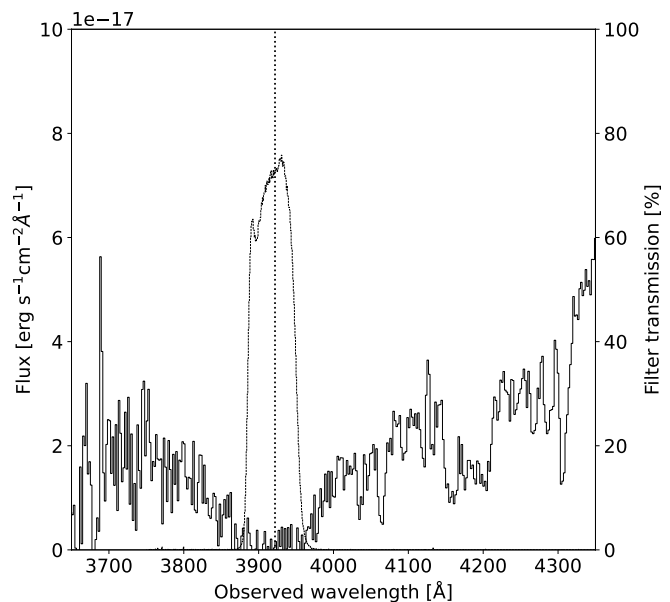


Fig. 1. Region around the DLA in the spectrum of Q 1218+0832 shown together with the filter transmission curve (dotted line) of the 63  -wide narrow-band filter NB391_7 used in this study (see also Fig. 2 in Geier et al. (2019)). The vertical dotted line shows the expected position of Lyman- α at the redshift of $z = 2.2261$ measured from low-ionisation metal lines in Geier et al. (2019). The filter, although designed for other purposes, matches the DLA trough perfectly.

The data from the NOT were reduced and combined using standard procedures for bias subtraction, flat-fielding, and im-

Table 1. Log of ALFOSC and OSIRIS observations.

Observation	Date	Exposure time (sec)
ALFOSC/NB391_7	20/03/2023	5×3000
ALFOSC/NB391_7	22/03/2023	2×3000
ALFOSC/g	20/03/2023	5×200
ALFOSC/g	22/03/2023	5×200
ALFOSC/r	20/03/2023	5×200
ALFOSC/r	22/03/2023	5×200
OSIRIS/R1000B	07/07/2023	2×1000

age combination implemented in a set of Python scripts. The code for image combination using sigma-clipping is available on GitHub¹. The combined seeing in the stacked images are 1.3, 1.2, and 1.2 arcsec for g, r, and NB391_7, respectively.

Unfortunately, no standard stars were observed on the nights of observation. However, based on the calibration described in Sect. 3, we estimate that the $3\text{-}\sigma$ detection limit in the narrow-band image is 3×10^{-17} erg s⁻¹ cm⁻².

The spectroscopic data were reduced using a set of Python scripts for the reduction of long-slit spectra. The code is available on GitHub². The spectrum was wavelength-calibrated using HgAr and Ne arc frames. The spectrum was flux-calibrated using observations of the spectrophotometric standard star Ross640 observed on the same night.

We also analysed public HST observations of the field taken with the Advanced Camera for Surveys (ACS) in the F814W filter as part of the Sloan Lens ACS (SLACS) Survey (SLACS) (Bolton et al. 2006). We obtained reduced data from the Hubble Legacy Archive³. The $3\text{-}\sigma$ detection limit in the image is 26.8 mag per arcsec² and the point spread function (PSF) has a full width at half maximum (FWHM) of 0.113 arcsec.

We note that three asteroids were detected in our NOT broad-band images: NR10, OU129, and SA197. All three have well-determined orbits.

3. Results

Fig. 2 shows the full field covered by our NOT images with the positions of objects discussed in the paper marked with arrows.

3.1. The DLA galaxy counterpart

In Fig. 3 we show a 32×32 arcsec² around Q 1218+0832 from our NOT imaging. The quasar is completely absent in the narrow-band image. A few nearby sources were detected in the narrow-band and broad-band images. Fig. 4 shows a 15×15 arcsec² zoom in on the region around Q 1218+0832 from the HST F814W image with the NB391_7 data overlaid as contours. Some of the weak contours from the NB391_7 image south of the quasar overlap with sources detected in the HST image. We need deeper narrow-band observations to establish if any of these sources are Lyman- α emitters at $z = 2.2261$.

In order to search for continuum emission from the galaxy counterpart of the DLA at a small impact parameter, we also attempted PSF subtraction in the HST image. We used GALFIT

(Peng et al. 2010) to fit and subtract a PSF defined by an unsaturated star in the field. In Fig. 5 we compare the result of the PSF subtraction for Q 1218+0832 with the results for a nearby star at RA(J2000.0) = 12:18:25.9, Dec(J2000.0)=+08:32:27.0 that is about 50% brighter than Q 1218+0832. This comparison allowed us to gauge the size of the systematic PSF-subtraction residuals. There is no convincing emission detected down to an impact parameter of about 0.3 arcsec (2.5 proper kpc at $z = 2.2261$). At smaller impact parameters, the PSF subtraction introduces substantial systematic errors, making it difficult to differentiate between PSF-subtraction residuals and potential genuine signals originating from the DLA galaxy and/or the quasar host galaxy.

3.2. Lyman- α emitters in the field

Although we could not derive a precise flux calibration of the NB391_7 image, we could still identify objects with a strong excess or a strong deficit of flux in the narrow band using the colour-colour diagrams as described in, for example, Møller & Warren (1993); Fynbo et al. (1999), and Fynbo et al. (2002).

Q 1218+0832 stands out as the object with the strongest narrow-band flux deficit. One object at RA(J2000) = 12:18:28.41, Dec(J2000)=+08:31:22.65 has a strong excess of emission in the narrow-band image as seen in Fig. 7. The object is marked as 'S' 59 arcsec south of Q 1218+0832 in Fig. 2. At $z = 2.23$, 59 arcsec correspond to 493 proper kpc. The object is very bright and can be seen in all the individual 3000-sec narrow-band exposures. No other emission line sources are detected above 5σ significance.

In Fig. 8 we overlaid the contours of the narrow-band image on top of the F814W ACS image. In the HST image, the source is only slightly larger than the PSF with a measured FWHM of 0.119 arcsec, whereas a PSF has a FWHM of 0.113 arcsec. The intrinsic size of the object must be only about 0.037 arcsec or 300 pc at $z = 2.2261$. In the narrow band, the source was also resolved, leading to an intrinsic size of about 4 kpc. Hence, the Lyman- α emission is much more extended than the continuum emission. This is something that is frequently seen for Lyman- α emitters at these redshifts (e.g. Møller & Warren 1998; Rauch et al. 2008; Steidel et al. 2011).

Assuming that most objects have an NB391_7 - g colour close to 0, we can get a rough flux calibration of the NB391_7 image. Under this assumption, the emission line source has a magnitude of NB391_7(AB) \approx 22.8. The broad-band magnitudes are $g(AB) = 24.38\pm 0.11$ and $r(AB) = 24.46\pm 0.18$ measured in a large circular aperture with a 3 arcsec radius. The HST image gives consistent results for the F814W filter: AB = 24.32 ± 0.06 . Given the estimate of the NB391_7(AB) magnitude, the flux and luminosity for the emission line source can be estimated using the formulae provided in Fynbo et al. (2002). The flux is estimated to be close to 3×10^{-16} erg s⁻¹ cm⁻² and the luminosity close to 1.3×10^{43} erg s⁻¹.

A spectrum was secured in July despite somewhat poor visibility. In the spectrum, shown in Fig. 9, we detected a single bright emission line at 3937.8 ± 0.4 Å, which nominally was redshifted by 1218 km s⁻¹ relative to Lyman- α at $z = 2.2261$. The inset in Fig. 9 shows the profile of the line. Due to resonant scattering, the Lyman- α line is often asymmetric and with a double horn profile (Neufeld 1990; Laursen et al. 2009; Verhamme et al. 2018) and the systemic redshift of the galaxy can therefore not be accurately determined from the centre of the Lyman- α line, which can be redshifted by up to at least 1500 km s⁻¹ (Shap-

¹ <https://github.com/jfynbo/Pyclip>

² <https://github.com/keheintz/PyReduc>

³ <https://hla.stsci.edu>

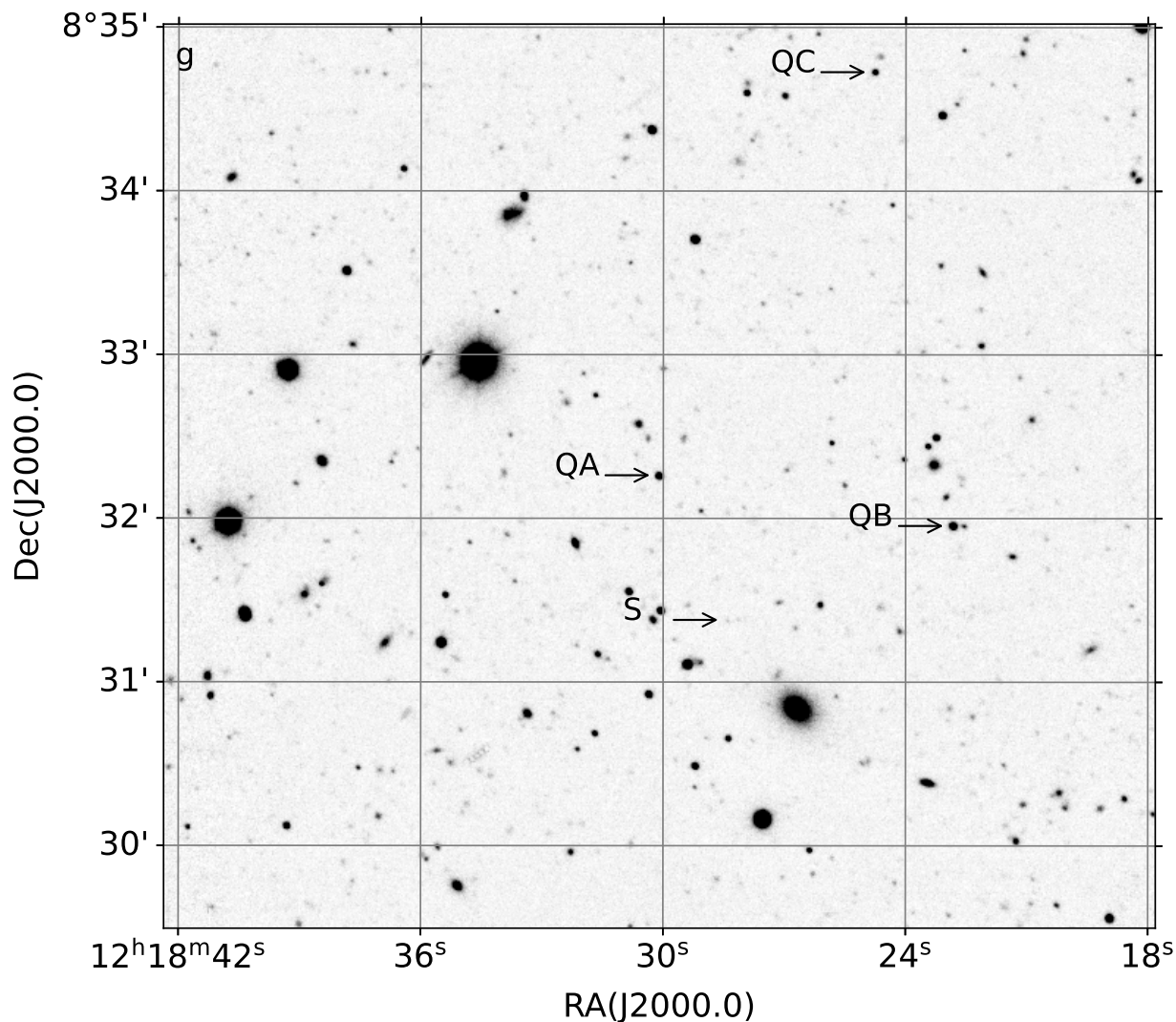


Fig. 2. Full g-band image around Q 1218+0832 (marked 'QA'). The field of view is 6.0×5.4 arcmin². North is up and east is to the left. Other objects marked are discussed further in the text: a Lyman- α emitter marked 'S', and two other quasars are marked 'QB' and 'QC'.

ley et al. 2003). To measure the systemic redshift of the galaxy, we need measurements of restframe optical emission lines such as Balmer lines or [O III] lines that can be observed in the near-infrared. The flux of the line is 2.5×10^{-16} erg s⁻¹ cm⁻², which is in good agreement with the estimated flux from the narrow-band imaging given the uncertainty in the narrow-band calibration and the effect of slit loss.

3.3. Other objects of interest in the field

There is another quasar in the field, namely SDSS J121822.83+083157.0 (marked 'QB' in Fig. 2). This quasar is at nearly the same redshift as Q 1218+0832 ($z = 2.637$ vs $z = 2.60$ for Q 1218+0832) and has a separation of 109 arcsec from Q 1218+0832 and 90 arcsec from the emission line source. Converted to physical distances at $z = 2.23$, the distance between the two quasar sight lines is 899 proper kpc.

In the spectrum of SDSS J121822.83+083157.0 (shown in Fig. 10), there is no metal absorption at $z = 2.2261$ down to a $3\text{-}\sigma$ observed equivalent width limit of 0.6 Å. There is also no strong absorption in the Lyman- α forest at this redshift. As shown in the inset in Fig. 10, there is Lyman- α absorption just a few hundred

km s⁻¹ blueshifted and redshifted relative to $z = 2.2261$, but this is neither damped nor strong enough to be from a Lyman-limit system (LLS). Rather than absorption, there seems to be an island of high transmission at $z = 2.2261$.

Furthermore, we note that Richards et al. (2009) classified the object SDSS J121824.76+083443.5 as a quasar with a photometric redshift of $z = 2.245$ (marked 'QC' in Fig. 2). This object is located 168 arcsec north of Q 1218+0832. The upper and lower values for the photometric redshift estimate are by Richards et al. (2009) and were determined to be $z_L = 2.040$ and $z_U = 2.630$, respectively. Hence, the object may well be unrelated to the DLA, but it would be interesting to measure the spectroscopic redshift for this source to establish if it is part of the same structure as the DLA or possibly is at the same redshift as the two other quasars. If it is at a larger redshift of the DLA, the spectrum could still be used to look for intervening absorption at $z = 2.2261$ – the redshift of the DLA towards Q 1218+0832. We note that the object has neither been detected by Gaia nor by the Wide-field Infrared Survey Explorer (WISE) (Secretst et al. 2015; Gaia Collaboration et al. 2023).

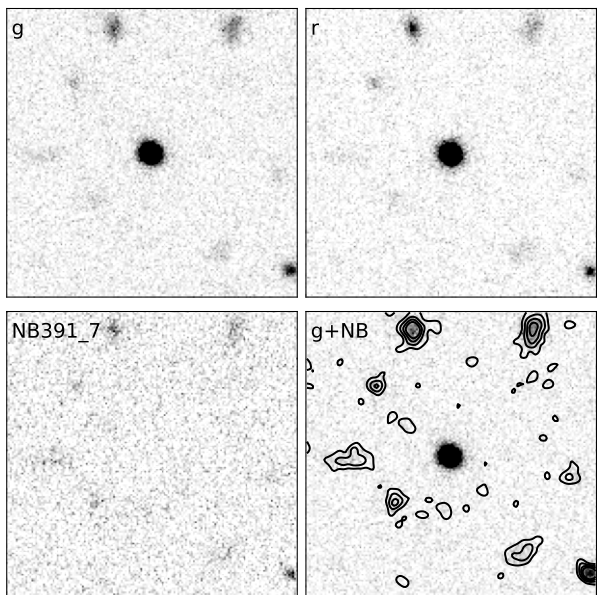


Fig. 3. 32×32 arcsec² region around Q 1218+0832. In the top row, we show the broad-band g and r images. The bottom left image shows the NB391_7 image. In the bottom right image, we overplotted the contours of the NB391_7 image smoothed by a Gaussian kernel with a width equal to the seeing on top of the g-band image. We note that the quasar is undetected in the NB391_7 image.

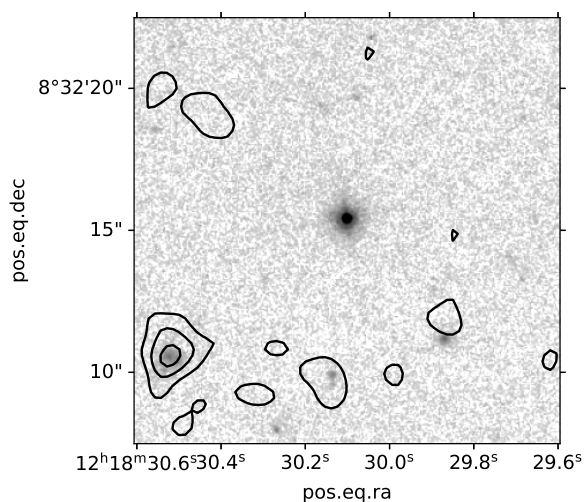


Fig. 4. DLA region (15×15 arcsec²). The underlying image is the HST F814W image. The contours are from the narrow-band image smoothed by a Gaussian kernel with width matched to the seeing.

4. Discussion

4.1. The DLA

The neutral hydrogen in the structures traced by DLAs is so large, more specifically similar to the amount of baryons we find in stars in local galaxies, that DLA must represent an important ingredient in the galaxy formation recipe (Wolfe 1986). However, the precise manner in which this ingredient should be added to the recipe is still not fully understood. The absorption characteristics of DLAs as they are imprinted on the light of the background quasars are very similar to the characteristics of the absorption seen in gamma-ray burst (GRB) afterglows, which we know result from absorption in the interstellar medium

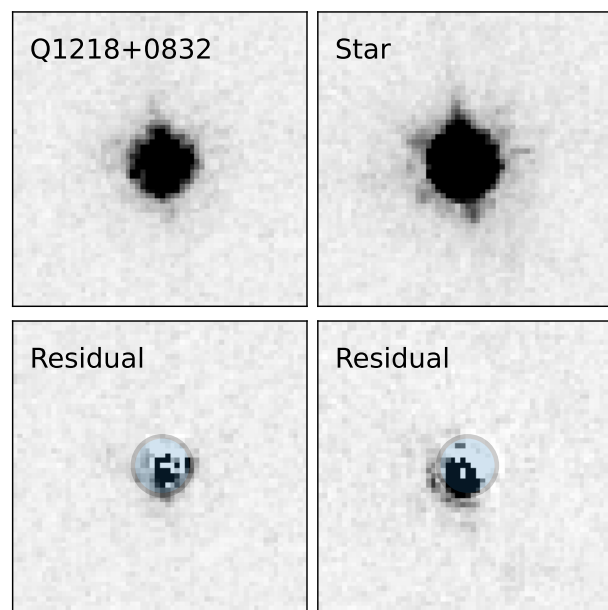


Fig. 5. 3×3 arcsec² region before (top row) and after (bottom row) PSF subtraction. The two left columns show Q 1218+0832 and the two right columns show another point source that is about 50% brighter than Q 1218+0832. There is no significant excess emission outside of 0.3 arcsec from the quasar (marked by a circle in the lower row).

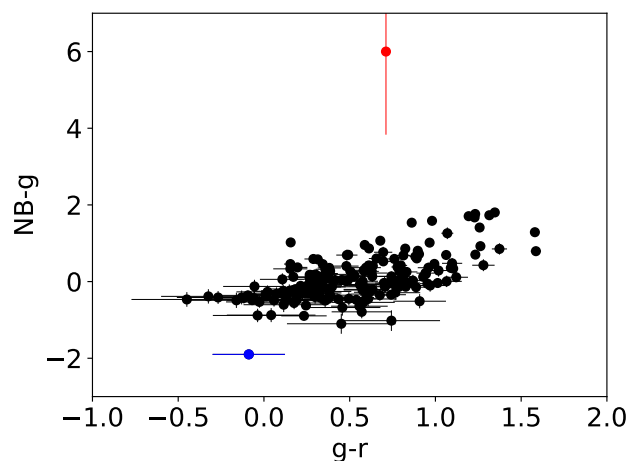


Fig. 6. Colour-colour diagram based on the NOT imaging in the g and r filters and the NB391_7 filter. Two objects stand out, namely Q 1218+0832 (marked in red), which has a deficit of flux in the narrow filter, and an emission line source, marked in blue, with excess emission in the narrow filter.

(ISM) of star-forming galaxies (e.g. Jensen et al. 2001; de Ugarte Postigo et al. 2018, and many similar cases). The two classes of absorbers also follow the same scaling relations (Arabsalmani et al. 2015). It is therefore plausible that DLAs must trace environments that are similar to the ISM of star-forming galaxies. It is possible to reconcile the absorption statistics of quasar and GRB absorbers in a simple model where they are drawn from the same underlying sample of star-forming galaxies at $z > 2$ (Fynbo et al. 2008; Krogager et al. 2020). DLAs also allow us to trace important scaling relations (Møller et al. 2013; Christensen et al. 2014; Rhodin et al. 2018). Getting similarly detailed information, for example, about chemical abundances for galax-

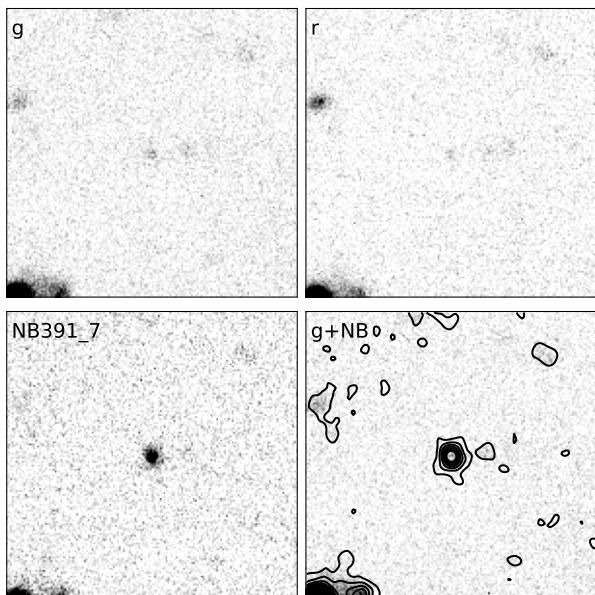


Fig. 7. 32×32 arcsec² region around the position of the strong emission line source we detect 90 arcsec south of Q 1218+0832. In the top row, we show the broad-band g and r images. The bottom left image shows the NB391_7 image. In the bottom right image, we overplotted linearly spaced contours of the NB391_7 image smoothed by a Gaussian kernel with a width equal to the seeing on top of the g-band image.

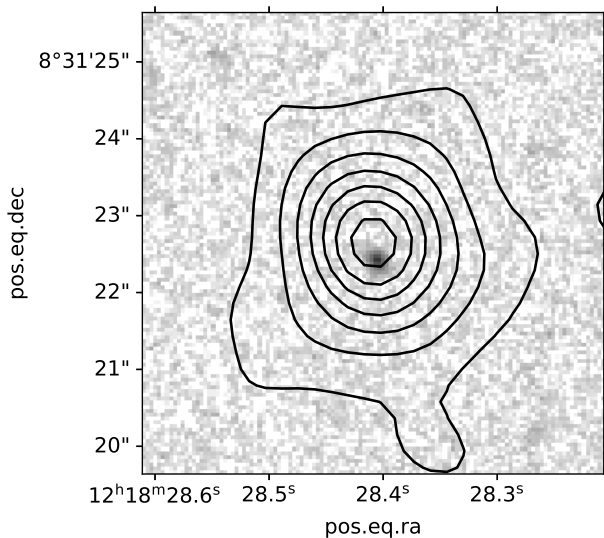


Fig. 8. 6×6 arcsec² region around the emission line source. The underlying image is the HST F814W image. The contours are from the narrow-band image smoothed by a Gaussian kernel with a width matched to the seeing. The contour levels are linearly spaced.

ies detected in emission would be either impossible or extremely expensive.

The amount of neutral hydrogen in DLAs and sub-DLAs show hardly any evolution over a wide redshift range from 5 to 0 (Prochaska & Wolfe 2009; Noterdaeme et al. 2009, 2012; Zafar et al. 2013; Crighton et al. 2015). Therefore, it is not the case that there is a one-to-one correspondence between the baryons seen as DLAs at $z > 2$ and the baryons found inside stars in the local Universe. Maybe DLAs represent a mix of absorption in the ISM phase as well as absorption from cold gas in circum-galactic material (CGM). The CGM component can itself be a mix of

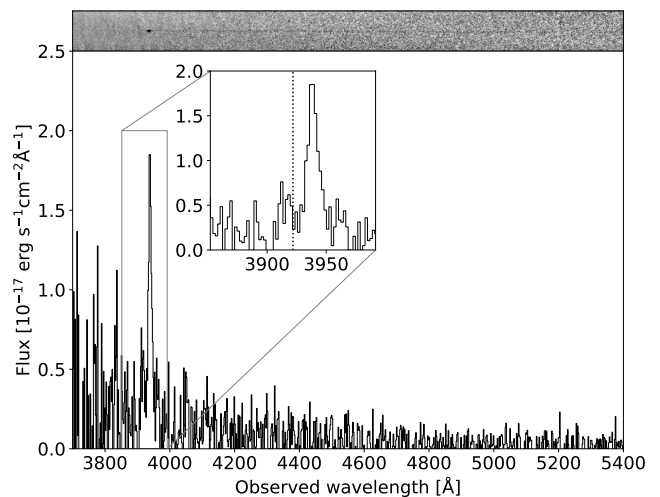


Fig. 9. Blue end of the OSIRIS/R1000B spectrum of the bright Lyman- α marked S in Fig. 2. The top panel shows the two-dimensional spectrum and the bottom panel the extracted one-dimensional spectrum. A single bright emission line was detected at 3937.8 ± 0.4 Å on top of a blue continuum. The inset shows a zoom-in on the line where the dotted line shows the position of Lyman-alpha centred at $z = 2.2261$.

material accreting onto the dark matter halo of the galaxy and material leaving the host in the form of a galactic wind. Such a scenario seems to be supported by simulations of DLAs (Pontzen et al. 2008; Altay et al. 2013; Bird et al. 2014; Sommer-Larsen & Fynbo 2017; Rhodin et al. 2019).

It is important to locate more galaxy counterparts of DLAs as this is the best way to gain insight into how DLAs in the real Universe concretely are related to the galaxies we see in emission. Furthermore, for the issue of dust bias, we would like to know which sight lines are most likely to significantly redden and obscure background sources as in the case Q 1218+0832 and other similar cases. In the last dozen years, good progress has been made in finding galaxy counterparts of DLAs, especially when focussing on metal-rich DLAs. Krogager et al. (2020) represent the most recent compilation of detections. This compilation, which includes 21 systems, shows that DLA galaxies follow correlations between the impact parameter of the galaxy and the line of sight to the background quasar: more metal-rich galaxies tend to have larger impact parameters and DLAs with larger H I column densities tend to have smaller impact parameters.

The galaxy counterpart of the DLA towards Q 1218+0832 remains undetected. There is nothing seen in narrow-band imaging (albeit shallow) and nothing in the HST image at impact parameters $0.3 < b < 5$ arcsec (corresponding to about 2.5 – 40 kpc). Both from the modelling and from the observed sample in Krogager et al. (2020), we expect the counterpart of the DLA towards Q 1218+0832 to be located at a small impact parameter - due to its very large H I column density. The presence of C I and CO absorption also supports a small impact parameter (Krogager & Noterdaeme 2020), but we do note that cold gas was also detected in the $z = 2.583$ DLA towards Q 0918+1636 that is located at an impact parameter of 2.0 arcsec (16 kpc). The galaxy is not a strong Lyman- α emitter; otherwise, it would have shown up both in the long-slit spectroscopy presented in paper I and in the narrow-band imaging presented here. The most promising outlook for detecting the galaxy is either through near-infrared spectroscopy, which would allow the detection of H α or [O III] emission as for the DLAs towards Q 0918+1636 (Fynbo et al. 2013, neither of which are bright in Lyman- α emis-

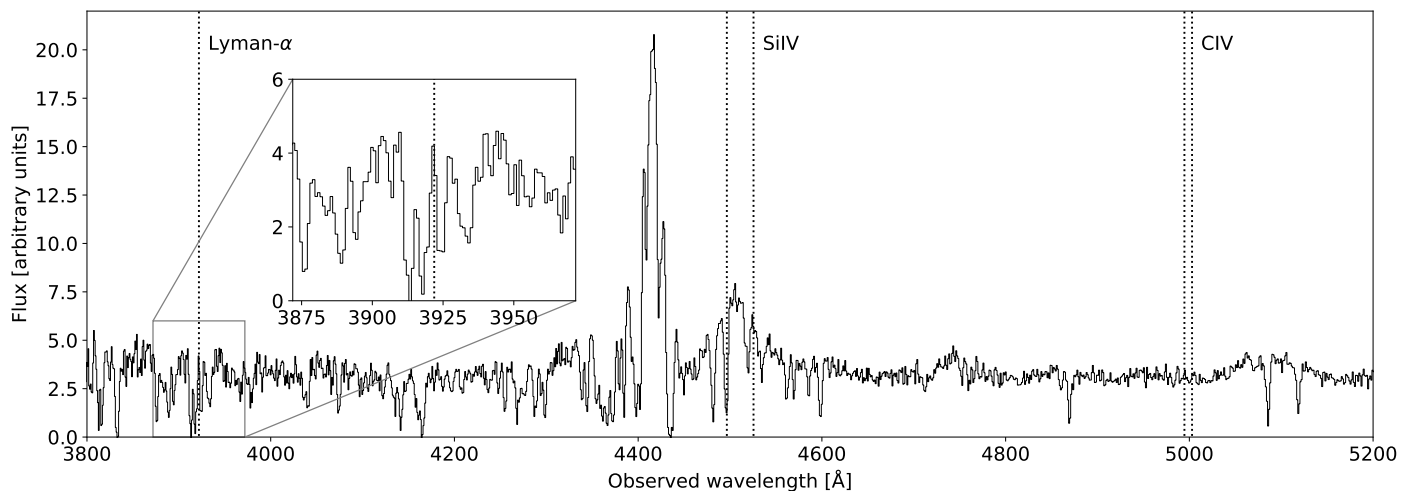


Fig. 10. Section of the SDSS spectrum of the $z = 2.637$ quasar SDSS J121822.83+083157.0 ('QB' in Fig. 2) located 109 arcsec west of Q 1218+0832 ('QA' in Fig. 2). Vertical lines indicate the expected positions of H I, Si IV, and C IV absorption lines at the redshift of the DLA, $z = 2.2261$. The inset shows a zoom-in on the region around Lyman- α . No significant absorption was detected at that redshift. The metal lines seen in the spectrum are from an associated $z_{abs} > z_{em}$ system at $z = 2.650$.

sion), or with the Atacama Large Millimeter/submillimeter Array (ALMA) where the galaxy could show up in CO emission as in the case of J2225+0527 (Kanekar et al. 2020), which is detected in CO(3-2) emission at an impact parameter of 5.6 kpc.

It is interesting that the quasar is completely absent in the narrow-band imaging. We can use this to draw conclusions about the transverse size of the DLA. If there really is no emission detectable with the NB391_7 filter, the DLA must cover not only the quasar broad line region but also the quasar host galaxy (assuming that the host has emission at 1090 Å, which is the wavelength probed by the NB391_7 filter at the redshift of Q 1218+0832). Of course, we need deeper imaging to infer if this is indeed the case.

Systems such as Q 1218+0832 and its intervening DLA show that the dust reddening of quasars and other distant sources due to dust in the foreground objects discussed by Ostriker & Heisler (1984) is a real effect. We note that the upcoming Purely Astrometric Quasar Survey (PAQS Krogager et al. 2023) will be able to determine quantitatively how strong the effect is, that is, what the frequency is for significant reddening and dimming of background quasars due to dust in foreground galaxies.

4.2. The environment

Even though we have not been able to locate the DLA galaxy, we have gained new insights into its environment. We detected a single bright emission line source 59 arcsec (corresponding to 493 proper kpc at $z = 2.2261$) south of Q 1218+0832. The source is among the brightest Lyman- α emitters at similar redshifts (compare, e.g. with the samples in Fynbo et al. 2002; Nilsson et al. 2009; Sandberg et al. 2015; Matthee et al. 2021). It would be interesting to secure a significantly deeper image in the NB391_7 filter to reach the flux level of more typical Lyman- α emitters and hence be able to infer more about the galaxy density in the field. Comparing to the sample of Nilsson et al. (2009) (in particular their fig. 3), it is clear that source S is at the absolute bright end of the luminosity function for Lyman- α and that more typical galaxies (in that study) are about 2 magnitudes fainter. Previous studies of Lyman- α emitters in the fields of high-column density H I absorbers have found an indication of filamentary structures

or galaxy overdensities (e.g. Møller & Warren 1998; Møller & Fynbo 2001; Fynbo et al. 2003; Lofthouse et al. 2023). In the case of Q 0918+1636, a bright CO emitter was detected at a distance of 117 kpc from the DLA galaxy (Fynbo et al. 2018). If DLA galaxies are frequently located in dense galaxy fields, this could help explain the surprisingly large correlation length of DLAs (Pérez-Ràfols et al. 2018). A preference for DLAs in group environments could result from tidal stripping of neutral gas out of galaxies in such environments (See also Bouché et al. 2012, 2013; Rauch et al. 2016).

The environment can also be probed by the multiple sight lines offered by at least two quasars in the field (the quasar nature of SDSS J121824.76+083443.5 remains to be established by spectroscopy). There is no metal-line absorption at $z = 2.2261$ in the spectrum of the $z = 2.637$ quasar SDSS J121822.83+083157.0. In the Lyman- α forest, there is no absorption exactly at $z = 2.2261$, but some forest lines are slightly blueshifted and redshifted relative to that redshift. D'Odorico et al. (2002) studied ten similar cases of multiple nearby quasar sight lines and detected five out of ten matching systems of strong absorption systems within 1000 km s⁻¹, indicating an overdensity of strong absorption systems over separation lengths from 1 to 8 h⁻¹ Mpc. More recently, Urbano Stawinski et al. (2023) have studied a larger sample of 32 DLAs intersecting close pairs of quasars. Their sample probes smaller impact parameters out to about 300 kpc. At these distances, there is a covering factor of > 90% for C IV and > 50% for strong H I absorbers (LLSs and DLAs). Similar studies have been carried out testing the covering factor of C IV absorption around Lyman-break galaxies and Lyman- α emitters (Adelberger et al. 2005; Bielby et al. 2017; Muzahid et al. 2021; Dutta et al. 2021; Banerjee et al. 2023; Galbiati et al. 2023). These studies have found excess C IV absorption at distances of a few hundred proper kiloparsecs.

5. Conclusions

The objective of this paper is to present new information about the dusty $z = 2.2261$ DLA towards the reddened quasar Q 1218+0832. This information constitutes of two main parts. Concerning the galaxy counterpart of the DLA, we have anal-

ysed new narrow-band observations and archival HST imaging to place strong constraints on its properties. It is most likely located at a very low impact parameter of $b < 0.3$ arcsec (or < 2.5 proper kpc at $z = 2.2261$). Concerning the environment of the DLA galaxy, we have shown that there is at least one other galaxy nearby, namely a bright Lyman- α emitter that is located 59 arcsec towards the south at a projected distance of 493 proper kpc at $z = 2.2261$. The environment can be further probed using sight lines to another quasar in the field 109 arcsec towards the west (899 proper kpc at $z = 2.2261$) and here there is no metal or strong H I absorption at the redshift of the DLA. A third quasar in the field has not been observed spectroscopically, but the photometric redshift evidence suggests that it could either be at the same redshift as the DLA or at a higher redshift and hence it can be used to further probe the environment of the DLA.

Further spectroscopic observations are required to search for the DLA galaxy at small impact parameters, to measure the precise redshift of the Lyman- α emitter, and to establish the relation of the third quasar to the environment of the DLA.

Acknowledgements. We thank an anonymous referee for a very helpful report. JPUF thanks Claudio Grillo for his advice about the HST observations. Based on observations made with the Gran Telescopio Canarias (GTC) and with the Nordic Optical Telescope (NOT), installed at the Spanish Observatorio del Roque de los Muchachos belonging to the Instituto de Astrofísica de Canarias. Also based on observations made with the NASA/ESA Hubble Space Telescope, and obtained from the Hubble Legacy Archive, which is a collaboration between the Space Telescope Science Institute (STScI/NASA), the Space Telescope European Coordinating Facility (ST-ECF/ESA) and the Canadian Astronomy Data Centre (CADM/NRC/CSA). Funding for the Sloan Digital Sky Survey V has been provided by the Alfred P. Sloan Foundation, the Heising-Simons Foundation, the National Science Foundation, and the Participating Institutions. SDSS acknowledges support and resources from the Center for High-Performance Computing at the University of Utah. The SDSS web site is www.sdss.org. SDSS is managed by the Astrophysical Research Consortium for the Participating Institutions of the SDSS Collaboration, including the Carnegie Institution for Science, Chilean National Time Allocation Committee (CNTAC) ratified researchers, the Gotham Participation Group, Harvard University, Heidelberg University, The Johns Hopkins University, L'École polytechnique fédérale de Lausanne (EPFL), Leibniz-Institut für Astrophysik Potsdam (AIP), Max-Planck-Institut für Astronomie (MPIA Heidelberg), Max-Planck-Institut für Extraterrestrische Physik (MPE), Nanjing University, National Astronomical Observatories of China (NAOC), New Mexico State University, The Ohio State University, Pennsylvania State University, Smithsonian Astrophysical Observatory, Space Telescope Science Institute (STScI), the Stellar Astrophysics Participation Group, Universidad Nacional Autónoma de México, University of Arizona, University of Colorado Boulder, University of Illinois at Urbana-Champaign, University of Toronto, University of Utah, University of Virginia, Yale University, and Yunnan University. The Cosmic Dawn Center (DAWN) is funded by the Danish National Research Foundation under grant No. 140. JPUF is supported by the Independent Research Fund Denmark (DFR-4090-00079) and thanks the Carlsberg Foundation for support. LC is supported by the Independent Research Fund Denmark (DFR-2032-00071). KEH acknowledges support from the Carlsberg Foundation Reintegration Fellowship Grant CF21-0103.

References

Adelberger, K. L., Shapley, A. E., Steidel, C. C., et al. 2005, *ApJ*, 629, 636
 Altay, G., Theuns, T., Schaye, J., Booth, C. M., & Dalla Vecchia, C. 2013, *MNRAS*, 436, 2689
 Arabsalmani, M., Møller, P., Fynbo, J. P. U., et al. 2015, *MNRAS*, 446, 990
 Banerjee, E., Muzahid, S., Schaye, J., Johnson, S. D., & Cantalupo, S. 2023, arXiv e-prints, arXiv:2304.04788
 Beaver, E. A., Burbidge, E. M., McIlwain, C. E., Epps, H. W., & Strittmatter, P. A. 1972, *ApJ*, 178, 95
 Bielby, R. M., Shanks, T., Crighton, N. H. M., et al. 2017, *MNRAS*, 471, 2174
 Bird, S., Vogelsberger, M., Haehnelt, M., et al. 2014, *MNRAS*, 445, 2313
 Bolton, A. S., Burles, S., Koopmans, L. V. E., Treu, T., & Moustakas, L. A. 2006, *ApJ*, 638, 703
 Bouché, N., Hohensee, W., Vargas, R., et al. 2012, *MNRAS*, 426, 801
 Bouché, N., Murphy, M. T., Kacprzak, G. G., et al. 2013, *Science*, 341, 50
 Christensen, L., Møller, P., Fynbo, J. P. U., & Zafar, T. 2014, *MNRAS*, 445, 225

Crighton, N. H. M., Murphy, M. T., Prochaska, J. X., et al. 2015, *MNRAS*, 452, 217
 de Ugarte Postigo, A., Thöne, C. C., Bolmer, J., et al. 2018, *A&A*, 620, A119
 D'Odorico, V., Petitjean, P., & Cristiani, S. 2002, *A&A*, 390, 13
 Dutta, R., Fumagalli, M., Fossati, M., et al. 2021, *MNRAS*, 508, 4573
 Ellison, S. L., Yan, L., Hook, I. M., et al. 2001, *A&A*, 379, 393
 Fynbo, J. P. U., Geier, S. J., Christensen, L., et al. 2013, *MNRAS*, 436, 361
 Fynbo, J. P. U., Heintz, K. E., Neeleman, M., et al. 2018, *MNRAS*, 479, 2126
 Fynbo, J. P. U., Krogager, J. K., Heintz, K. E., et al. 2017, *A&A*, 606, A13
 Fynbo, J. P. U., Laursen, P., Ledoux, C., et al. 2010, *MNRAS*, 408, 2128
 Fynbo, J. P. U., Ledoux, C., Møller, P., Thomsen, B., & Burud, I. 2003, *A&A*, 407, 147
 Fynbo, J. P. U., Møller, P., Thomsen, B., et al. 2002, *A&A*, 388, 425
 Fynbo, J. P. U., Prochaska, J. X., Sommer-Larsen, J., Dessauges-Zavadsky, M., & Møller, P. 2008, *ApJ*, 683, 321
 Fynbo, J. U., Møller, P., & Warren, S. J. 1999, *MNRAS*, 305, 849
 Gaia Collaboration, Vallenari, A., Brown, A. G. A., et al. 2023, *A&A*, 674, A1
 Galbati, M., Fumagalli, M., Fossati, M., et al. 2023, *MNRAS*, 524, 3474
 Geier, S. J., Heintz, K. E., Fynbo, J. P. U., et al. 2019, *A&A*, 625, L9
 Gupta, N., Srianand, R., Shukla, G., et al. 2021, *ApJS*, 255, 28
 Haehnelt, M. G., Steinmetz, M., & Rauch, M. 2000, *ApJ*, 534, 594
 Kneib, K. E., Fynbo, J. P. U., Ledoux, C., et al. 2018, *A&A*, 615, A43
 Jensen, B. L., Fynbo, J. U., Gorosabel, J., et al. 2001, *A&A*, 370, 909
 Jorgenson, R. A. & Wolfe, A. M. 2014, *ApJ*, 785, 16
 Jorgenson, R. A., Wolfe, A. M., Prochaska, J. X., et al. 2006, *ApJ*, 646, 730
 Kanekar, N., Prochaska, J. X., Neeleman, M., et al. 2020, *ApJ*, 901, L5
 Kaur, B., Kanekar, N., Revalski, M., et al. 2022, *ApJ*, 934, 87
 Koo, D. C. 1986, in *Astrophysics and Space Science Library*, Vol. 122, Spectral Evolution of Galaxies, ed. C. Chiosi & A. Renzini, 419–438
 Krogager, J. K., Fynbo, J. P. U., Heintz, K. E., et al. 2016a, *ApJ*, 832, 49
 Krogager, J.-K., Fynbo, J. P. U., Møller, P., et al. 2019, *MNRAS*, 486, 4377
 Krogager, J. K., Fynbo, J. P. U., Noterdaeme, P., et al. 2016b, *MNRAS*, 455, 2698
 Krogager, J. K., Leighly, K. M., Fynbo, J. P. U., et al. 2023, *The Messenger*, 190, 38
 Krogager, J.-K., Møller, P., Christensen, L. B., et al. 2020, *MNRAS*, 495, 3014
 Krogager, J. K., Møller, P., Fynbo, J. P. U., & Noterdaeme, P. 2017, *MNRAS*, 469, 2959
 Krogager, J.-K. & Noterdaeme, P. 2020, *A&A*, 644, L6
 Laursen, P., Razoumov, A. O., & Sommer-Larsen, J. 2009, *ApJ*, 696, 853
 Ledoux, C., Petitjean, P., Fynbo, J. P. U., Møller, P., & Srianand, R. 2006, *A&A*, 457, 71
 Lofthouse, E. K., Fumagalli, M., Fossati, M., et al. 2023, *MNRAS*, 518, 305
 Lu, L., Sargent, W. L. W., Barlow, T. A., Churchill, C. W., & Vogt, S. S. 1996, *ApJS*, 107, 475
 Mackenzie, R., Fumagalli, M., Theuns, T., et al. 2019, *MNRAS*, 487, 5070
 Matthee, J., Sobral, D., Hayes, M., et al. 2021, *MNRAS*, 505, 1382
 Møller, P., Christensen, L., Zwaan, M. A., et al. 2018, *MNRAS*, 474, 4039
 Møller, P., Fynbo, J. P. U., & Fall, S. M. 2004, *A&A*, 422, L33
 Møller, P., Fynbo, J. P. U., Ledoux, C., & Nilsson, K. K. 2013, *MNRAS*, 430, 2680
 Møller, P. & Fynbo, J. U. 2001, *A&A*, 372, L57
 Møller, P. & Warren, S. J. 1993, *A&A*, 270, 43
 Møller, P. & Warren, S. J. 1998, *MNRAS*, 299, 661
 Muzahid, S., Schaye, J., Cantalupo, S., et al. 2021, *MNRAS*, 508, 5612
 Neeleman, M., Kanekar, N., Prochaska, J. X., et al. 2017, *Science*, 355, 1285
 Neufeld, D. A. 1990, *ApJ*, 350, 216
 Nilsson, K. K., Tapken, C., Møller, P., et al. 2009, *A&A*, 498, 13
 Noterdaeme, P., Petitjean, P., Carithers, W. C., et al. 2012, *A&A*, 547, L1
 Noterdaeme, P., Petitjean, P., Ledoux, C., & Srianand, R. 2009, *A&A*, 505, 1087
 Ostriker, J. P. & Heisler, J. 1984, *ApJ*, 278, 1
 Partridge, R. B. & Peebles, P. J. E. 1967, *ApJ*, 147, 868
 Pei, Y. C., Fall, S. M., & Hauser, M. G. 1999, *ApJ*, 522, 604
 Peng, C. Y., Ho, L. C., Impey, C. D., & Rix, H.-W. 2010, *AJ*, 139, 2097
 Pérez-Ràfols, I., Font-Ribera, A., Miralda-Escudé, J., et al. 2018, *MNRAS*, 473, 3019
 Péroux, C., Bouché, N., Kulkarni, V. P., York, D. G., & Vladilo, G. 2011, *MNRAS*, 410, 2237
 Péroux, C. & Howk, J. C. 2020, *ARA&A*, 58, 363
 Pontzen, A., Governato, F., Pettini, M., et al. 2008, *MNRAS*, 390, 1349
 Prochaska, J. X. & Wolfe, A. M. 2009, *ApJ*, 696, 1543
 Rauch, M., Becker, G. D., & Haehnelt, M. G. 2016, *MNRAS*, 455, 3991
 Rauch, M., Haehnelt, M., Bunker, A., et al. 2008, *ApJ*, 681, 856
 Rhodin, N. H. P., Agertz, O., Christensen, L., Renaud, F., & Fynbo, J. P. U. 2019, *MNRAS*, 488, 3634
 Rhodin, N. H. P., Christensen, L., Møller, P., Zafar, T., & Fynbo, J. P. U. 2018, *A&A*, 618, A129
 Richards, G. T., Myers, A. D., Gray, A. G., et al. 2009, *ApJS*, 180, 67
 Sadler, E. M., Moss, V. A., Allison, J. R., et al. 2020, *MNRAS*, 499, 4293

- Sandberg, A., Guaita, L., Östlin, G., Hayes, M., & Kiaerød, F. 2015, *A&A*, 580, A91
- Schaye, J. 2001, *ApJ*, 559, L1
- Schmidt, M. 1963, *Nature*, 197, 1040
- Secrest, N. J., Dudik, R. P., Dorland, B. N., et al. 2015, *ApJS*, 221, 12
- Shapley, A. E., Steidel, C. C., Pettini, M., & Adelberger, K. L. 2003, *ApJ*, 588, 65
- Sommer-Larsen, J. & Fynbo, J. P. U. 2017, *MNRAS*, 464, 2441
- Stecher, T. P. 1965, *ApJ*, 142, 1683
- Steidel, C. C., Bogosavljević, M., Shapley, A. E., et al. 2011, *ApJ*, 736, 160
- Steidel, C. C., Giavalisco, M., Pettini, M., Dickinson, M., & Adelberger, K. L. 1996, *ApJ*, 462, L17
- Urbano Stawinski, S. M., Rubin, K. H. R., Prochaska, J. X., et al. 2023, *arXiv e-prints*, arXiv:2305.11232
- Verhamme, A., Garel, T., Ventou, E., et al. 2018, *MNRAS*, 478, L60
- Wild, V. & Hewett, P. C. 2005, *MNRAS*, 361, L30
- Wolfe, A. M. 1986, *Philosophical Transactions of the Royal Society of London Series A*, 320, 503
- Wolfe, A. M., Gawiser, E., & Prochaska, J. X. 2005, *ARA&A*, 43, 861
- Wolfe, A. M., Turnshek, D. A., Smith, H. E., & Cohen, R. D. 1986, *ApJS*, 61, 249
- Zafar, T., Péroux, C., Popping, A., et al. 2013, *A&A*, 556, A141

GQ 1218+0832, SDSS J121822.83+083157.0,
SDSS J121824.76+083443.5, NR10, OU129, SA197